

# Imaging visible light using anisotropic metamaterial slab lens

Jie Yao,<sup>1,7</sup> Kun-Tong Tsai,<sup>2,7</sup> Yuan Wang,<sup>1,7</sup> Zhaowei Liu,<sup>3</sup> Guy Bartal,<sup>1</sup>  
Yuh-Lin Wang,<sup>2,4,6</sup> and Xiang Zhang<sup>1,5\*</sup>

<sup>1</sup>National Science Foundation (NSF) Nanoscale Science and Engineering Center (NSEC), 5130 Etcheverry Hall, University of California, Berkeley, CA 94720–1740, USA

<sup>2</sup>Institute of Atomic and Molecular Sciences, Academia Sinica, Taiwan P.O. box 23-166, Taipei 10617, Taiwan

<sup>3</sup>Department of Electrical & Computer Engineering, University of California, San Diego, La Jolla, California 92093, USA

<sup>4</sup>Department of Physics, National Taiwan University, Taipei 106, Taiwan

<sup>5</sup>Materials Sciences Division, Lawrence Berkeley National Laboratory, 1 Cyclotron Road, Berkeley, CA 94720, USA

<sup>6</sup>These authors contributed equally to this work.

<sup>7</sup>ylwang@pub.iam.s.sinica.edu.tw

\*xiang@berkeley.edu

**Abstract:** It has been shown that an anisotropic metamaterial made of nanowire array can realize negative refraction of light even without a negative phase index of refraction. Such non-resonant bulk material can be fabricated by bottom-up electrochemical method. Using this material, we were able to achieve lensing action with micron-thick slab and demonstrate imaging of a slit object. The details of the focused light beam in 3-dimensional space have been mapped with near field scanning optical microscope (NSOM).

©2009 Optical Society of America

OCIS codes: (160.3918) Metamaterials; (110.0110) Imaging systems.

---

## References and links

1. D. R. Smith, J. B. Pendry, and M. C. K. Wiltshire, "Metamaterials and negative refractive index," *Science* **305**(5685), 788–792 (2004) (and the references therein.).
2. R. Wangberg, J. Elser, E. E. Narimanov, and V. A. Podolskiy, "Nonmagnetic nanocomposites for optical and infrared negative-refractive-index media," *J. Opt. Soc. Am. B* **23**(3), 498–505 (2006).
3. M. G. Silveirinha, P. A. Belov, and C. R. Simovski, "Subwavelength imaging at infrared frequencies using an array of metallic nanorods," *Phys. Rev. B* **75**(3), 035108 (2007).
4. J. Yao, Z. Liu, Y. Liu, Y. Wang, C. Sun, G. Bartal, A. M. Stacy, and X. Zhang, "Optical negative refraction in bulk metamaterials of nanowires," *Science* **321**(5891), 930 (2008).
5. Y. Liu, G. Bartal, and X. Zhang, "All-angle negative refraction and imaging in a bulk medium made of metallic nanowires in the visible region," *Opt. Express* **16**(20), 15439–15448 (2008).
6. S. Zhang, W. Fan, N. C. Panoiu, K. J. Malloy, R. M. Osgood, and S. R. J. Brueck, "Experimental demonstration of near-infrared negative-index metamaterials," *Phys. Rev. Lett.* **95**(13), 137404 (2005).
7. A. N. Grigorenko, A. K. Geim, H. F. Gleeson, Y. Zhang, A. A. Firsov, I. Y. Khrushchev, and J. Petrovic, "Nanofabricated media with negative permeability at visible frequencies," *Nature* **438**(7066), 335–338 (2005).
8. V. M. Shalaev, W. S. Cai, U. K. Chettiar, H. K. Yuan, A. K. Sarychev, V. P. Drachev, and A. V. Kildishev, "Negative index of refraction in optical metamaterials," *Opt. Lett.* **30**(24), 3356–3358 (2005).
9. G. Dolling, C. Enkrich, M. Wegener, C. M. Soukoulis, and S. Linden, "Simultaneous negative phase and group velocity of light in a metamaterial," *Science* **312**(5775), 892–894 (2006).
10. G. Dolling, M. Wegener, C. M. Soukoulis, and S. Linden, "Negative-index metamaterial at 780 nm wavelength," *Opt. Lett.* **32**(1), 53–55 (2007).
11. J. Valentine, S. Zhang, T. Zentgraf, E. Ulin-Avila, D. A. Genov, G. Bartal, and X. Zhang, "Three Dimensional Optical Metamaterial Exhibiting Negative Refractive Index," *Nature* **455**(7211), 376–379 (2008).
12. M. Stockman, "Criterion for Negative Refraction with Low Optical Losses from a Fundamental Principle of Causality," *Phys. Rev. Lett.* **98**(17), 177404 (2007).
13. D. R. Smith, and D. Schurig, "Electromagnetic wave propagation in media with indefinite permittivity and permeability tensors," *Phys. Rev. Lett.* **90**(7), 077405 (2003).
14. V. G. Veselago, "The electrodynamics of substances with simultaneously negative values of  $\epsilon$  and  $\mu$ ," *Sov. Phys. Usp.* **10**(4), 509–514 (1968).
15. C. Y. Liu, A. Datta, and Y. L. Wang, "Ordered Anodic Alumina Nano-channels on Focused-Ion-beam Prepatterned Aluminum Surfaces," *Appl. Phys. Lett.* **78**(1), 120–122 (2001).

16. G. Riveros, S. Green, A. Cortes, H. Gómez, R. E. Marotti, and E. A. Dalchiele, "Silver nanowire arrays electrochemically grown into nanoporous anodic alumina templates," *Nanotechnology* **17**(2), 561–570 (2006).
  17. G. L. Hornyak, C. J. Patrissi, and C. R. Martin, "Fabrication, Characterization, and Optical Properties of Gold Nanoparticle/Porous Alumina Composites: The Nonscattering Maxwell–Garnett Limit," *J. Chem. Phys. B* **101**(9), 1548–1555 (1997).
  18. K. H. A. Lau, L. Tan, K. Tamada, M. S. Sander, and W. Knoll, "Highly Sensitive Detection of Processes Occurring Inside Nanoporous Anodic Alumina Templates: A Waveguide Optical Study," *J. Chem. Phys. B* **108**(30), 10812–10818 (2004).
  19. P. B. Johnson, and R. W. Christy, "Optical Constants of the Noble Metals," *Phys. Rev. B* **6**(12), 4370–4379 (1972).
  20. C. A. Foss, G. L. Hornyak, J. A. Stockert, and C. R. Martin, "Template-synthesized nanoscopic gold particles: optical spectra and the effects of particle size and shape," *J. Phys. Chem.* **98**(11), 2963–2971 (1994).
  21. N. Fang, H. Lee, C. Sun, and X. Zhang, "Sub-diffraction-limited optical imaging with a silver superlens," *Science* **308**(5721), 534–537 (2005).
  22. Z. Liu, H. Lee, Y. Xiong, C. Sun, and X. Zhang, "Far-field optical hyperlens magnifying sub-diffraction-limited objects," *Science* **315**(5819), 1686 (2007).
- 

## 1. Introduction

The traditional perception of positive index of refraction has been recently shattered by the introduction of a set of artificial materials with the ability to refract light in anomalous ways. The routes to such materials include the design of simultaneous existence of negative permittivity ( $\epsilon$ ) and permeability ( $\mu$ ) [1], and a non-magnetic approach which implements the strong anisotropy of the materials [2–5]. The former approach has so far gained great success in a broad range of electromagnetic wave frequencies from microwave (GHz) range to infrared region [6–11]. However, for even higher frequencies, such as visible light, the requirements of making such metamaterials becomes challenging, as it is difficult to fabricate deep-subwavelength features (as required by the definition of metamaterials) at large scales. Another major restriction to this kind of material is the high loss associated with the magnetic response that typically occurs at the resonance of the metallic structures [12]. Previously, we have experimentally demonstrated a new approach to achieve the negative refraction from the artificial anisotropy of metamaterials, which does not require any response or resonance to the magnetic component of electromagnetic waves [4]. The bottom-up method makes the fabrication in large scale possible and convenient.

Anisotropy induced negative refraction brings a new perspective to the design of metamaterials. The new metamaterial was made up of aligned silver nanowires, with diameter around 50nm and spacing about 110nm, inside porous alumina matrix in a self-organized hexagonal lattice. At the long wavelength limit, this metamaterial can be characterized as an effective uniaxial material with effective permittivity parallel to the nanowire being negative, and that perpendicular to the wire is positive [2,13]. This property extends over a very broad frequency range, (visible to near-infrared) and results in hyperbolic equifrequency contour (EFC) for a transverse magnetic (TM)-polarized light in the  $k_x, k_z$  plane (we define z axis along the nanowires. The light propagates in x-z plane.) Figures 1(a) presents a TM wave incident from free space and experiences negative refraction in the metamaterial as shown by the negative direction of Poynting vector  $S_r$  compared to the incident light. The phase front still propagates in the positive direction. On the other side the light will also experience negative refraction when it propagates from the metamaterial into air. This forms a slab lens as proposed by Vesalago in the 1960's [14]. Here we report the first experimental observation of lensing action of such a flat slab of metamaterials. We show that a slit object on the surface of this metamaterial slab can form an image outside the lens due to the negative refraction.

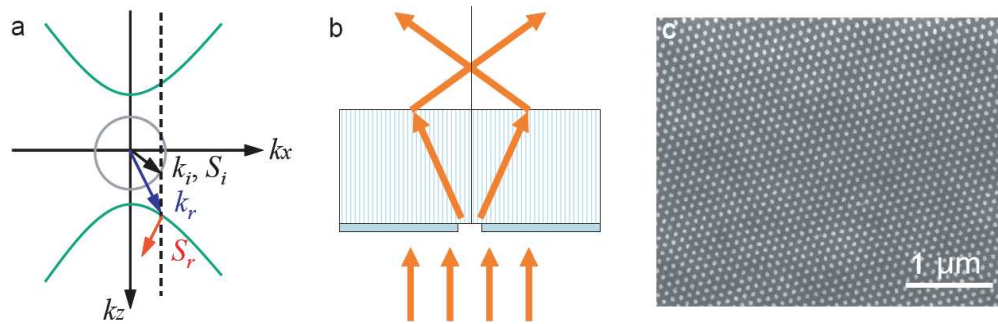


Fig. 1. (a) The equipfrequency contour (EFC) for a TM-polarized light is hyperbolic in the  $k_x, k_z$  plane, assuming the light propagation is centered along the wire (the  $z$ -axis). The grey circle is the EFC in air. The tangential component along the metamaterial/air interface is conserved. The direction change from the Poynting vector  $S_i$  to  $S_r$  shows the negative refraction. (b) Schematic picture showing the principle of imaging by a slab lens made of metamaterial with negative refraction ability. (c) Scanning electron microscope (SEM) image of the slab lens (top view). The center to center distance between nanowires is about 110nm in average.

## 2. Fabrication

The flat slabs of metamaterial for lensing action were fabricated by growing Ag into arrays of long-range ordered nanochannels in anodic aluminum oxide (AAO) templates. The process for preparing the substrates has been described previously [15]. Briefly, a finely polished aluminum foil was first exposed to a 50 keV Ga focused ion beam with a diameter of 10 nm to form an array of hexagonally closed-packed nano-concaves on its surface. The patterned substrate was then anodized in 0.3M oxalic acid. The positions of the nanochannels formed in the anodization are pinned by the nano-concaves, resulting in an array with well defined lattice spacing (110 nm) and extremely narrow pore size distribution. After removing the underlying aluminum substrate by a mixture of  $\text{CuCl}_2$  and HCl, the barrier layer at the bottom of the nanochannels was dissolved in diluted  $\text{H}_3\text{PO}_4$ . Subsequently, a layer of gold (400 nm) was deposited onto the bottom side of the free-standing AAO to form electrode, which facilitates the growth of silver into the nanochannels and the formation of a long-range ordered array of nanowires [16]. The final step of the process involved chemical mechanical polishing of the slab's top surface to ensure its flatness. Figure 1(c) depicts the scanning electron microscope (SEM) image of the slab lens (top view). Such an array of nanowires imbedded in the AAO formed a metamaterial slab working at wavelengths down to the visible range.

## 3. Experiment

We have used a  $4\mu\text{m}$  thick slab with a 600nm wide slit, cut through the gold seed layer, being the object. The slit was illuminated with a He-Ne laser at 633nm, where the polarization of the incident light can be selected by a linear polarizer. The transmitted light was mapped by NSOM in various distances from the output surface, using a tapered optical fiber coated with chromium as the NSOM tip. An aperture is drilled at the end of the tapered tip for light collection. A xyz AFM scanner was used to control the tip position so light in any point of interest in the 3D free space can be detected, which enables us to study the detail of the light profile at various distances from the output surface of the metamaterial slab. A schematic of the optical setup is shown in Fig. 2.

Figure 3(a) shows the cross sectional view of the light profile in the plane perpendicular to the slit. The light distribution in the space has been recovered by combining all the optical signals obtained by NSOM in each point at different heights. The bottom of the image is the output surface of the metamaterial slab. The light transmitted through the slit has been spread out into  $1.5\mu\text{m}$  wide at output surface. However, due to the transition from material with hyperbolic EFC to that with normal dielectric properties, the light divergence inverts into

convergence at the metamaterial-air interface. Consequently, the 600nm slit is retrieved as an 800nm wide line at the image plane, which is about  $1.7\mu\text{m}$  away from the interface. Based on the focus position, we can estimate an effective (group) index of refraction for the slab lens to be  $-2.2$ . Since the nanowire material shows negative refraction ability over a wide range of frequencies [4], the lensing phenomena can also be achieved for a broad spectrum.

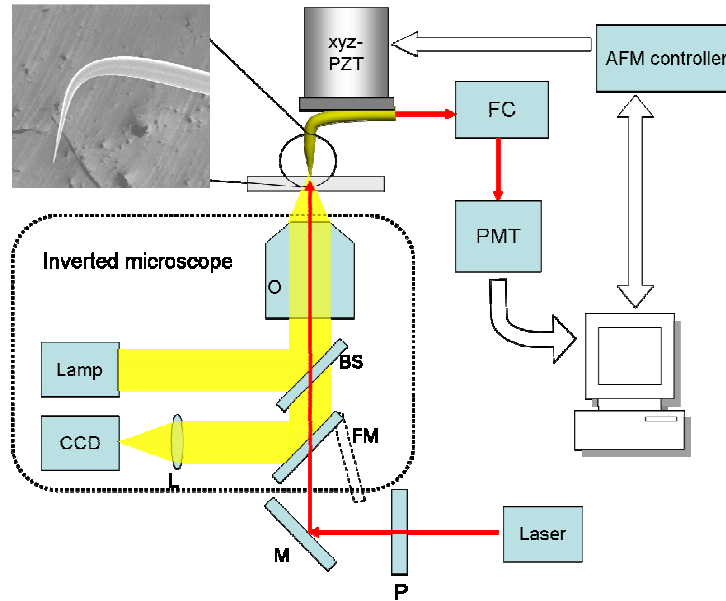


Fig. 2. Schematic of the optical set up. The sample was illuminated with a He-Ne laser at 633nm. The polarization of the incident light can be selected by a linear polarizer P. A flip mirror FM is used to enable the observation of the sample surface using CCD camera through the microscope objective lens O. The transmitted light was mapped by NSOM in various distances from the output surface, using a tapered optical fiber coated with chromium as the NSOM tip. The SEM image of the tip is shown in the up-left inset. A xyz AFM scanner was used to control the tip position so light in any point of interest in the 3D free space can be detected. The collected light is transmitted to a photo detector PMT through fiber coupler FC.

Numerical simulations using commercial software (CST Microwave studio) were conducted to verify the lensing action in the metamaterial slab. The parameters of the simulated structure are similar to those of the actual material properties with permittivities  $\epsilon = 2.4$  for the  $\text{Al}_2\text{O}_3$  [17,18] and  $\epsilon = -19.4 + 0.7i$  for Ag ([19,20] at wavelength of 633nm. The simulation results, shown in Fig. 3(c) reveal a  $0.8\mu\text{m}$  wide focused spot at  $2\mu\text{m}$  distance, similar to our experimental result. The inset in the picture gives the cross cuts of the intensity distribution at the focus point. The simulation result is consistent with the experiment. Also shown in this figure is the light propagating inside the metamaterial slab, which cannot be detected by the NSOM in our experiment. Incident light from the slit at the bottom gets diffracted, then re-focused after the refraction at the slab/air interface, just as shown in Fig. 1(b).

We note that the lensing action presented in this work is diffraction limited. Although the anisotropic metamaterial has the ability to support the propagation of high  $k$  component much larger than  $k_0$  (the wave vector of light in free space), those high  $k$  components are lost when the light is coupled back into the air, unlike the designs that enhance the evanescent waves [21,22]. The propagating light in air can only carry those components that are smaller than  $k_0$ , therefore, the focus point is diffraction limited no matter how narrow the original slit is.

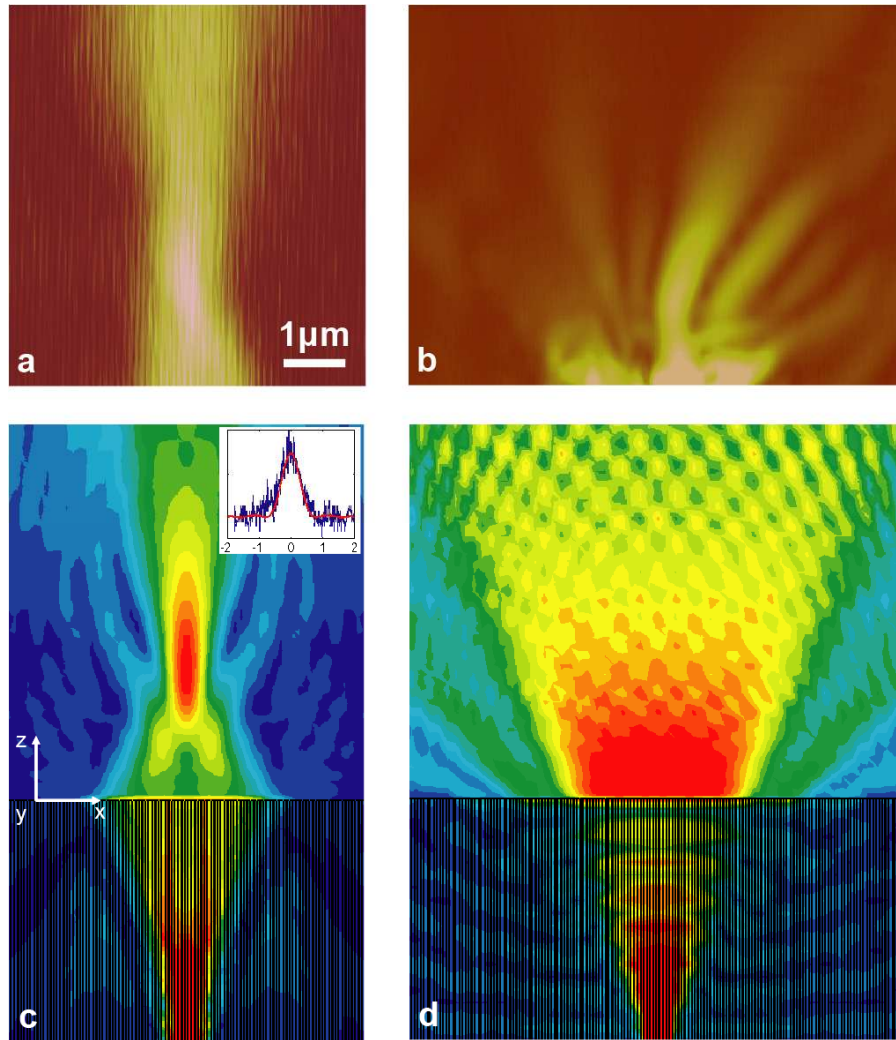


Fig. 3. Cross sectional view of the light profile in the  $xz$  plane which is perpendicular to the slit.  $y$ -axis is parallel to the slit. Incident light is propagating in  $z$  direction. (a) Focusing of TM polarized light. The light distribution in the space has been recovered by combining all the optical signals obtained by NSOM in each point at different heights. The noise level is higher than for TE wave due to higher loss and less transmission of TM wave comparing to TE wave. (b) NSOM measurement result of TE polarized light. The beam diverges after passing through the slab lens. No focusing effect is observed. The interference fringes are different from the simulation result due to the limitation of sample quality, NSOM resolution and sensitivity. (c)(d) Numerical simulation results for TM (c) and TE (d) polarized light in the cross sectional plane using commercial software (CST Microwave Studio). The lower part of (c) and (d) is the slab lens, where the nanowire array is shown. The upper part is air. The colors from blue to red in the simulation results represent increasing amplitude of electric component of the waves. The inset shows the cross cuts of the normalized intensity distribution at the focus point (Blue – experiment, Red - simulation). The unit of the horizontal axis is micrometer. (a), (b), (c) and (d) have the same scale bar.

It is worth pointing out that the focusing effect is polarization dependent. Since the hyperbolic EFC only applies to the TM mode of light, transverse electric (TE) light cannot be focused by the metamaterial slab in the way described above. As a control experiment, we have measured TE-polarized wave emerging from the metamaterial slab. The experimental result is shown in Fig. 3(b) and simulation result shown in Fig. 3(d). The light beam kept going broader and no focusing effect is observed.

In summary, we have successfully fabricated a slab lens using anisotropic metamaterial of nanowires. The imaging and focusing ability of the slab lens at 633nm wavelength has been demonstrated with the complete mapping of distribution of light in 3D space during the focusing process. Such a compact slab lens opens new opportunities for various applications such as imaging and lithography.

### **Acknowledgments**

This work was supported by the U. S. Army Research Office (ARO) MURI program 50432-PH-MUR and partly by the National Science Council (NSC95-3114-P-001-007-MY3) of Taiwan.